

01 May 2013, 2:00 pm - 4:00 pm

Calibration of Numerical Model for Liquefaction-Induced Effects on Levees and Embankments

Michelle Shriro
University of California, Berkeley, CA

Jonathan D. Bray
University of California, Berkeley, CA

Follow this and additional works at: <https://scholarsmine.mst.edu/icchge>



Part of the [Geotechnical Engineering Commons](#)

Recommended Citation

Shriro, Michelle and Bray, Jonathan D., "Calibration of Numerical Model for Liquefaction-Induced Effects on Levees and Embankments" (2013). *International Conference on Case Histories in Geotechnical Engineering*. 10.

<https://scholarsmine.mst.edu/icchge/7icchge/session01/10>



This work is licensed under a [Creative Commons Attribution-Noncommercial-No Derivative Works 4.0 License](#).

This Article - Conference proceedings is brought to you for free and open access by Scholars' Mine. It has been accepted for inclusion in International Conference on Case Histories in Geotechnical Engineering by an authorized administrator of Scholars' Mine. This work is protected by U. S. Copyright Law. Unauthorized use including reproduction for redistribution requires the permission of the copyright holder. For more information, please contact scholarsmine@mst.edu.

CALIBRATION OF NUMERICAL MODEL FOR LIQUEFACTION- INDUCED EFFECTS ON LEVEES AND EMBANKMENTS

Michelle Shriro

University of California
Berkeley, California-USA 94720

Jonathan D. Bray

University of California
Berkeley, California-USA 94720

ABSTRACT

Soil liquefaction presents a significant hazard to the built environment. The seismically induced permanent displacement of earth levees, dams, and embankments resulting from liquefaction below these earth structures is not well captured in current seismic design practice. The objective of this study is to advance the capabilities of numerical methods toward the solution of problems involving limited lateral spreads. The nonlinear soil constitutive model UBCSAND, as implemented in the finite difference program FLAC, (Itasca), is used to evaluate the seismic deformations of the newly-constructed Moss Landing Marine Laboratory (MLML) in Moss Landing, California resulting from liquefaction-induced lateral movements during the Loma Prieta earthquake of 1989. A material parameter selection protocol was developed through one-element modeling of laboratory testing and then implemented to predict deformations at the MLML facility.

INTRODUCTION

The liquefaction of soils presents a significant hazard to the built environment. Whereas much attention has been devoted over the past four decades towards developing liquefaction triggering procedures to evaluate the likelihood of liquefaction occurring, relatively less attention has been devoted to understanding liquefaction-induced ground movements.

Many of the prevalent procedures for evaluating liquefaction are discussed in the document "Recommended Procedures for Implementation of DMG Special Publication 117: Guidelines for Analyzing and Mitigating Liquefaction Hazards in California" edited by Martin and Lew (1999) and revised into SP117A by Parrish (2008). This important guidance document separates liquefaction-related slope movement hazards into two categories: 1) Flow slides wherein the post-liquefaction static factor of safety (FS) is below unity so that large displacements that are greater than a few meters occur after the cessation of earthquake shaking; and 2) "Limited" lateral spreads of the order of a meter or so triggered and sustained by the earthquake ground shaking."

Flow slides could potentially be the most catastrophic liquefaction-induced slope movement with an expected range of displacement typically on the order of several meters. Current prediction methods are well suited to predict their occurrence.

As summarized in Finn (1990), large liquefaction-induced levee crest settlements on the order of several meters are possible as the post-liquefaction factor of safety approaches a value of about 0.8. However, Finn also indicates that displacements of a meter or so are possible when the post-liquefaction factor of safety is slightly greater than one. Movements of a meter or so can produce significant damage to earth structures, so reliable procedures for estimating seismic displacements within this range of movements are also required. The seismically induced permanent displacement for these cases occurs primarily during earthquake shaking but after liquefaction is triggered. Hence, there are three important aspects of the problem to capture: (1) the point in which liquefaction is triggered; (2) the seismic response of the sliding mass during continued shaking; and (3) the post-liquefaction cyclic response of these soils. These are not easy aspects of nonlinear soil response to capture. Robust analytical procedures are required.

SOIL CONSTITUTIVE MODEL UBCSAND

Soil constitutive models have been developed in attempts to capture the cyclic response of soils undergoing cyclic mobility with limited strain potential in numerical simulations. The UBCSAND constitutive model is a nonlinear stress-dependent

effective stress model that captures the build-up of excess pore water pressure during cyclic loading and the development of “banana loops” in the shear stress versus shear strain plot once liquefaction occurs (e.g., Beaty and Byrne 1998, Byrne et al. 2004, and Park and Byrne 2004). Realistic soil responses are obtained by independently controlling the accumulation of permanent shear strains and volumetric strains in the model. It is one of the most popular nonlinear effective stress soil models used in engineering practice for evaluating liquefaction-induced deformation problems.

UBCSAND MODEL CALIBRATION PARAMETERS

Several versions of UBCSAND currently exist and the model is evolving continually. Thus, calibration of the UBCSAND model may vary with changes made to the model. The version of UBCSAND employed in this study was edited July 26, 2009. Model inputs includes parameters modeling elastic stiffness (Table 1), plastic shear stiffness (Table 2), strength, flow rule, relative density, and four fitting parameters. Through consultation with Professor Peter Byrne, the model developer, all but four fitting parameters controlling triggering and post-triggering dilation are correlated to the corrected standard penetration test (SPT) blow count value, referred to as $(N_1)_{60}$. The simplified correlations were evaluated for ability to capture and predict deformations by limiting required user input to SPT blow count and the four fitting parameters.

The constant volume friction angle is the parameter controlling the flow rule. Volumetric strain is calculated as a function of dilation angle. The dilation angle is calculated from the difference between peak friction angle and constant volume friction angle. The focus of this study was shear rather than volumetric deformations. A constant volume friction angle of 33 degrees is used while the peak friction angle is calculated as a function of constant volume friction angle and $(N_1)_{60}$ blow count. Correlation equations used in this study are provided in Table 3.

Table 1. Elastic Shear Stiffness Parameters and Corresponding Correlation Equations with $(N_1)_{60}$

Elastic Shear Stiffness Number (m_kge)	$m_kge = 21.7 \times 15((N_1)_{60})^{0.333}$
Maximum Shear Modulus (G_{\max})	$G_{\max} = m_kge \times P_{atm} \left(\frac{\sigma'_m}{P_{atm}} \right)^{m_ne}$
Bulk Stiffness Number (m_kb)	$m_kb = m_kge \times 0.916$
Bulk Modulus (K)	$K = m_kb \times P_{atm} \left(\frac{\sigma'_m}{P_{atm}} \right)^{m_me}$
Stress Exponents (m_ne, m_me)	$m_ne = 0.5, m_me = 0.5$

Table 2. Plastic Shear Stiffness Parameters and Corresponding Correlation Equations with $(N_1)_{60}$

Plastic Shear Modulus Number (m_kgp)	$m_kgp = [m_kge \times ((N_1)_{60})^2 \times 0.003] + 100$
Plastic Shear Modulus (G)	$G = m_kgp \times P_{atm} \left(\frac{\sigma'_m}{P_{atm}} \right)^{m_np}$
Plastic Shear Modulus Stress Exponent (m_np)	$m_np = 0.4$
Failure Ratio (m_rf)	$m_rf = 1.0 - \frac{m_n160}{100}$ where $0.5 < m_rf < 0.99$
Anisotropy Parameter ($m_anisofac$)	$m_anisofac = 0.0166 \times (N_1)_{60}$ where $0.333 < m_anisofac < 1.0$

Table 3. Plastic Shear Stiffness Parameters and Corresponding Correlation Equations with $(N_1)_{60}$

Constant Volume Friction Angle (m_phicv)	$m_phicv = 33$
Peak Friction Angle (m_phif)	$m_phif = m_phicv + \frac{(N_1)_{60}}{5.0}$

Four fitting parameters (m_hfac1 , m_hfac2 , m_hfac3 , and m_hfac4) are available within this version of UBCSAND. The parameter m_hfac3 was bypassed and set to 1 for this study. The other parameters will be further discussed in subsequent sections.

UBCSAND MODEL CALIBRATION WITH CSS LABORATORY TEST MODELING

The model input parameter accounting for the relative density of the soil is the corrected SPT blow count, or $(N_1)_{60}$ value. This parameter is in wide use in industry, though laboratory tests on which model calibrations are frequently based are typically performed using the measure of relative density. A common equation used to relate relative density with $(N_1)_{60}$ blow count is:

$$D_r = \sqrt{\frac{(N_1)_{60}}{C_d}} \quad (1)$$

As summarized in Idriss and Boulanger (2008), the value of C_d has been evaluated by numerous researchers and found to range between 35 and 65 for clean sands. A consistent conversion methodology was desirable to evaluate trends in

the fitting parameters. Initial modeling showed a value of 46 to be a value that could capture response of the majority of tests and was selected for this effort.

Representative cyclic simple shear (CSS) laboratory tests were selected and modeled using a single-element numerical simulation to evaluate the proficiency of the UBCSAND soil model. Laboratory CSS tests for sands were selected from data sets performed by Wu (2002) and Kammerer et al. (2002) on Monterey sand specimens and Nevada sand specimens, respectively. Several representative silt CSS tests were selected from data performed by Sancio (2003) and Arulmoli et al. (1992). These tests were used to evaluate the ability of the model to capture the cyclic pore water pressure increase and corresponding cyclic strain response in clean sand and silt soils. Laboratory tests were selected to represent flat and sloping ground conditions, and UBCSAND was then evaluated in terms of its ability to capture the seismic response of these test specimens under a range of densities, cyclic stress ratios, and initial static shear stresses.

Sand – Flat and Sloping Ground CSS Tests

Figures 1 and 2 show representative 4-way plots of shear stress vs. shear strain (upper left corner), shear stress vs. effective vertical stress (upper right corner), pore water pressure increase as a ratio of initial vertical effective stress vs. cycles of shear (lower left), and pore water pressure as a function of shear strain (lower right) for several CSS tests. Flat ground cases are presented on Figure 1 and are, in general, well matched. Damping is generally overestimated as can be seen by the difference in shapes of the ‘banana loops’ shown in the shear stress vs. shear strain plots.

Based on the tests modeled in this study, pore water pressures were typically overestimated by UBCSAND resulting in difficulty matching strains over a range of cycles (i.e., a range of approximately 5 to 20 cycles would represent typical earthquake scenarios possible in California). As an example of this, Figure 1 shows an overlay of predicted vs. actual laboratory results for Monterey Sand test MS23J. As a result of overestimation of pore water pressures, softening of soils occurs earlier in the time record than observed in the actual laboratory test. Looking at plots of shear stress vs. shear strain and effective vertical stress (the two upper plots), one can see that when sufficient softening has occurred to trigger yielding in the soil under cyclic loading, the initial predicted lateral yield is larger than measured but with additional cycles the strain increment is reduced relative to measured and a match can be achieved. The range of cycles over which a suitable match to measured strains can be achieved varies with relative density, CSR, initial static shear, plasticity, and other factors.

Figure 2 shows examples of calculated vs. measured response of clean sand specimens of Monterey and Nevada Sands under initial static loading conditions and subjected to cyclic loading in simple shear. The UBCSAND model can capture many key

aspects of soil response. However, it has a few limitations, which will be the focus of this discussion. Shear strain is typically only matched in the forward direction as can be seen for test NS3 and MS11J. Further, the model is unable to calculate accurately the significant shear strains that sometimes occur due to the static shear loading prior to the triggering of flow liquefaction but during the incremental building of pore water pressures. Specimen MS11J exhibits cyclic mobility with limited strain potential as well as incremental movements in the downslope direction (the direction of the initial static shear stress). We find that UBCSAND model can capture the deformation well once pore water pressures have incrementally increased to a pore water pressure ratio (R_u) of greater than about 50%. The UBCSAND model has not captured the effects of cyclic mobility with limited strain potential or the ‘creeping’ movements in the downslope direction driven by the initial static shear.

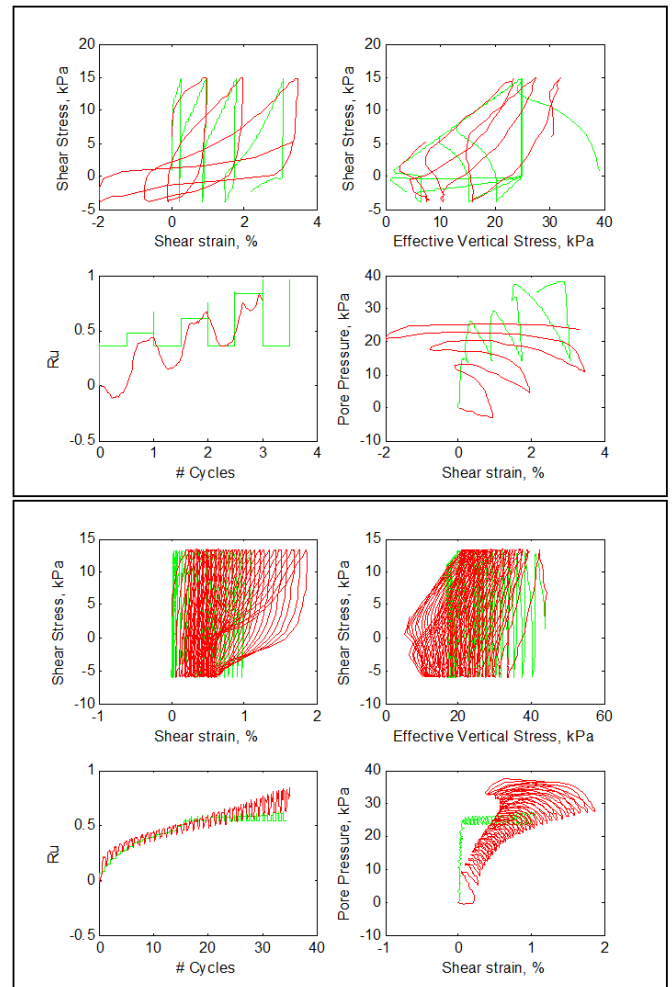


Fig. 1. Test data in red and UBCSAND output in green. Test MS19J (top): $\alpha=-0.01$; $D_r=55\%$; $CSR=.24$ (Wu, 2002). Test MS23J (bottom): $\alpha=0.006$; $D_r=81\%$; $CSR=0.20$ (Wu, 2002).

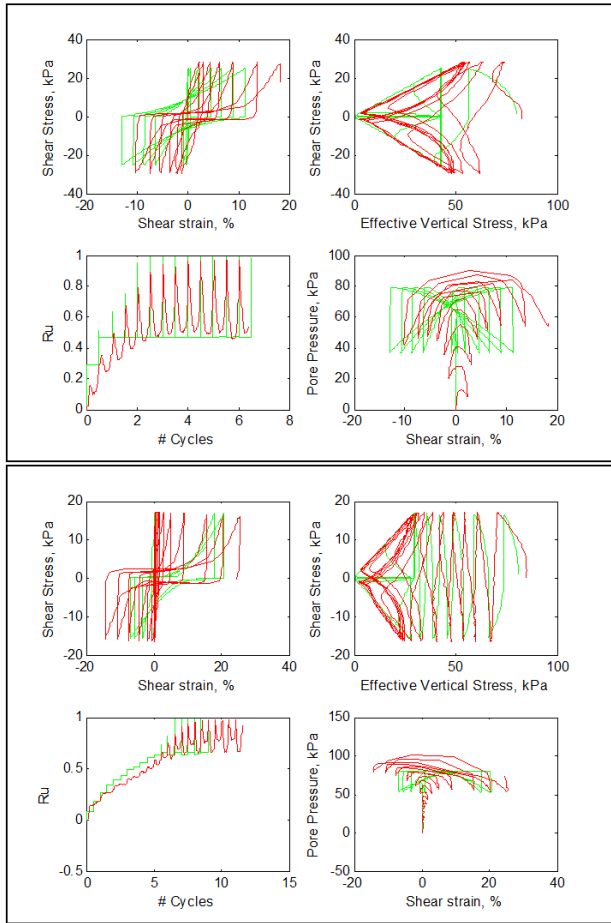


Fig. 2. Test data in red and UBCSAND output in green. Test NS3 (top): $\alpha=0.14$; $Dr=62\%$; $CSR=0.24$ (Kammerer, 2002). Test NS11J (bottom): $\alpha=0.08$; $Dr=90\%$; $CSR=0.22$ (Kammerer, 2002).

UBCSAND Fitting Parameters

In addition, to the UBCSAND model parameters that depend on conventional geotechnical characterizations (e.g., $(N_1)_{60}$), there are four “fitting” parameters that are available for use in UBCSAND. In this study, only two of these “fitting” parameters were used (i.e., m_{hfac1} and m_{hfac4}). The model parameters m_{hfac1} and m_{hfac2} were found to serve a similar function. Best results were obtained by setting the parameters equal to one another. These parameters are used to model the number of cycles to liquefaction and their value has an effect on the rate of pore water pressure rise with cyclic loading. Figure 3 shows values of m_{hfac1} and m_{hfac2} with the corrected SPT blow count, or $(N_1)_{60}$ value for sands and silts with a range of initial static shear stresses. Values of 0.5 to 2.0 were typical values used in our analyses, though values can be higher and lower than this range of values. For the case of sand at very low relative density, the value of m_{hfac1} (which is the same as m_{hfac2} for our study) must be increased to match liquefaction triggering response in CSS laboratory test results data. Increases in the initial static shear

stress acting on the soil yielded a weak trend of a corresponding increase in m_{hfac1} (and similarly, m_{hfac2}). The effect is most evident for sand at low relative density. Non-plastic or low plasticity silts were found to follow a similar trend to clean sands, though these materials required a slightly higher value of m_{hfac1} (and m_{hfac2}) to capture their measured cyclic response. As mentioned previously, the UBCSAND m_{hfac3} parameter was not used in this study and was set to 1. Lastly, the UBCSAND m_{hfac4} parameter was found to vary between approximately 0.5 and 2.5 for sands with typical values being between 1.5 and 2.0. The m_{hfac4} parameter was moderately influenced by the relative density of the sand at low CSR (i.e., $CSR \leq 0.2$) and by the value of the earthquake-induced CSR at higher CSR (i.e., $CSR \geq 0.2$). For silty soils, a value of 0.5 was selected for cases where the soil had a higher void ratio, and a value of 1.5 was selected for lower void ratio silty soils.

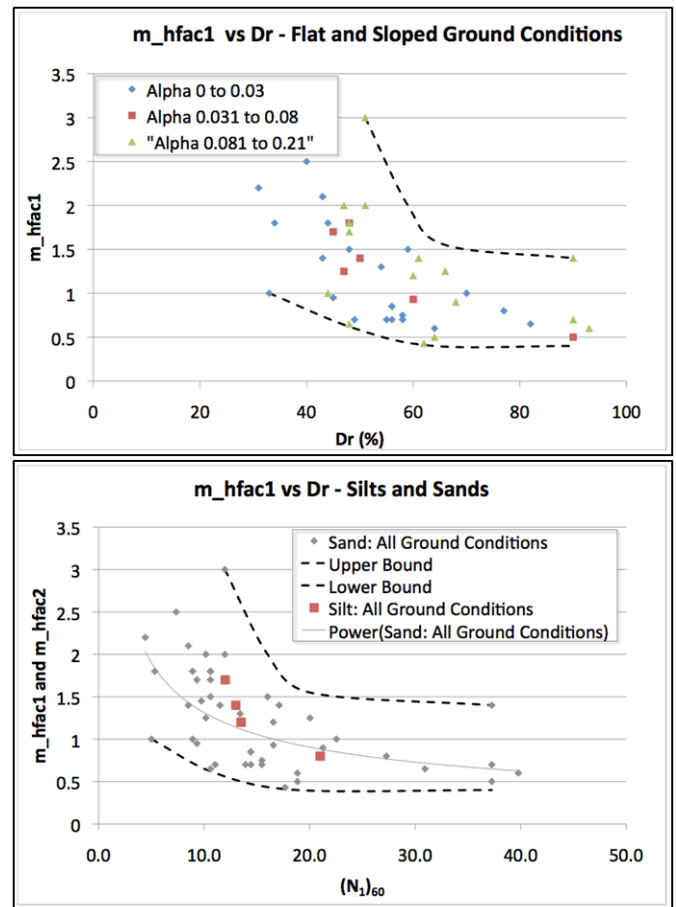


Fig. 3. Selected values of m_{hfac1} and m_{hfac2} found to yield a fit to the laboratory data.

UBCSAND MODEL

The former site of the Moss Landing Marine Laboratory lateral spread with a maximum displacement of 1.4 m during the 1989 Loma Prieta Earthquake was selected for back-

analysis with the UBCSAND model as implemented in FLAC to ensure that the analytical methods being employed in this research project provide reliable insights.

Moss Landing Marine Laboratory – Loma Prieta 1989

The Moss Landing Marine Laboratory (MLML) is located on the West side of Sandholdt road just south of the timber access bridge crossing the Old Salinas River in Moss Landing, California. The complex is shown on Figure 4 while photographs of racking of one of the structures and sand boil ejecta from an area just south of the structures are shown on Figure 5. The MLML facility consisted of three 1 to 2 story wood frame structures supported on spread footings constructed surrounding a center courtyard with appurtenant surface parking and a volleyball court to the south.

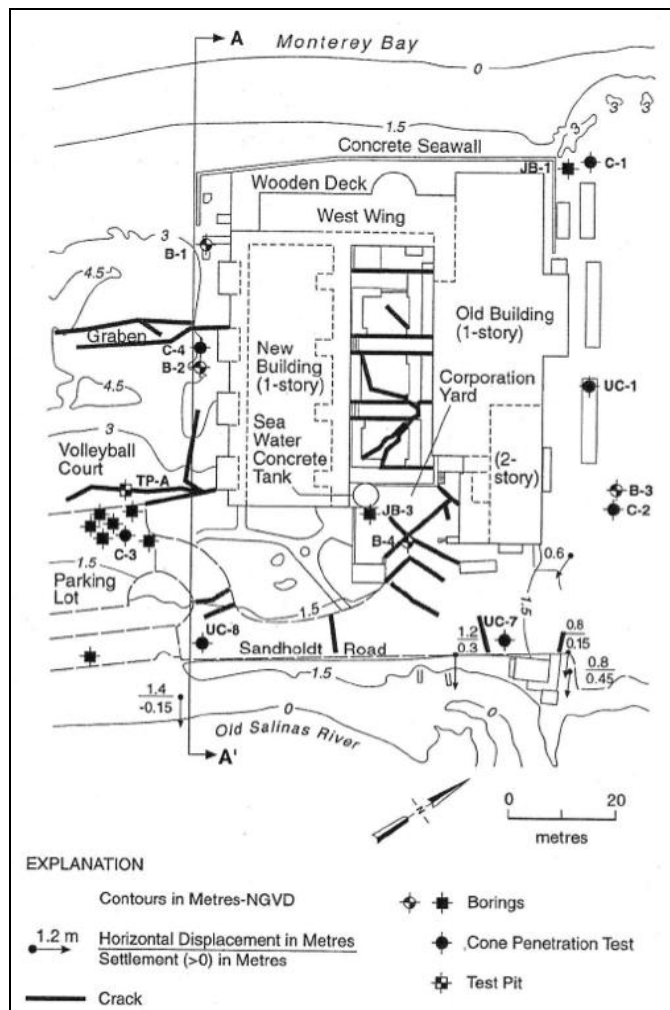


Fig. 4. Site map showing lateral spreading damage at the Moss Landing Marine Laboratory. (Boulanger et al. 1995).

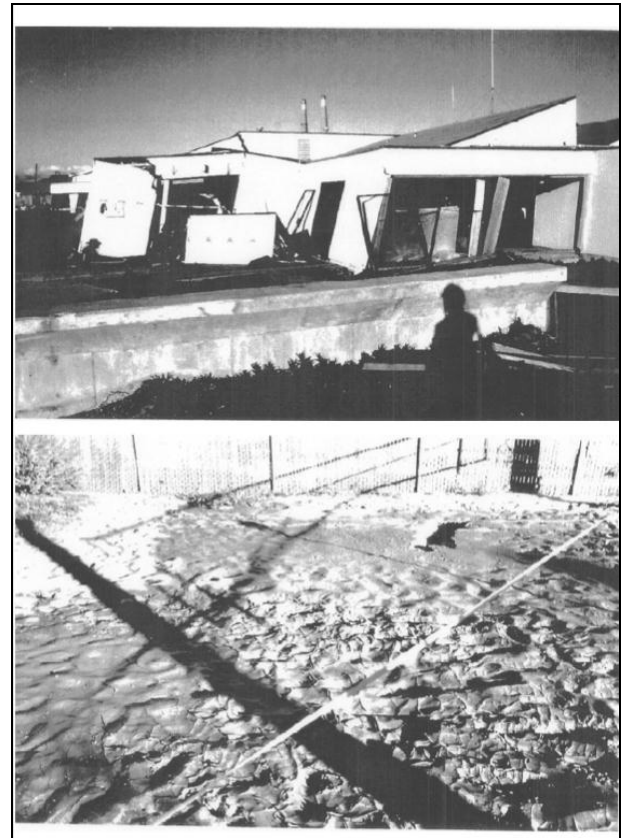


Fig. 5. Lateral spreading damage at the Moss Landing Marine Laboratory. Upper photo shows damage to the MLML structure. Lower photo shows sand boil ejecta at the volleyball court just south of the facility (Boulanger et al. 1995).

Site damage, subsurface stratigraphy, and a summary of available reports and information surrounding the case study were well documented and summarized in a comprehensive report by Boulanger et al. (1995). According to this report, sand boils were observed to have ejecta shooting several feet into the air for approximately 45 minutes after ground shaking associated with the Loma Prieta earthquake had ceased. Liquefaction and lateral spreading at the site had torn the structure apart, though it did not collapse. Lateral and vertical deformations were estimated in a post-earthquake survey by Brian Kangas Foulk and summarized in Boulanger et al. (1995). Geologic cross sections A-A' and B-B' (Figures 6 and 7, respectively) were prepared as part of the investigation led by Professor Boulanger. As summarized in Boulanger et al. (1995), the ground motion driving the observed lateral spread deformation was estimated to have a peak ground acceleration (PGA) of approximately 0.2 to 0.3 g using a bedrock motion of 0.15 g. The report concluded that 0.25 g would likely represent a median or slightly lower estimate of Loma Prieta earthquake. The Salinas ground motion record (PGA = 0.15 g) was identified as having similar soil conditions at depth and was scaled to 0.25 g. This ground motion was used as input in our analysis.

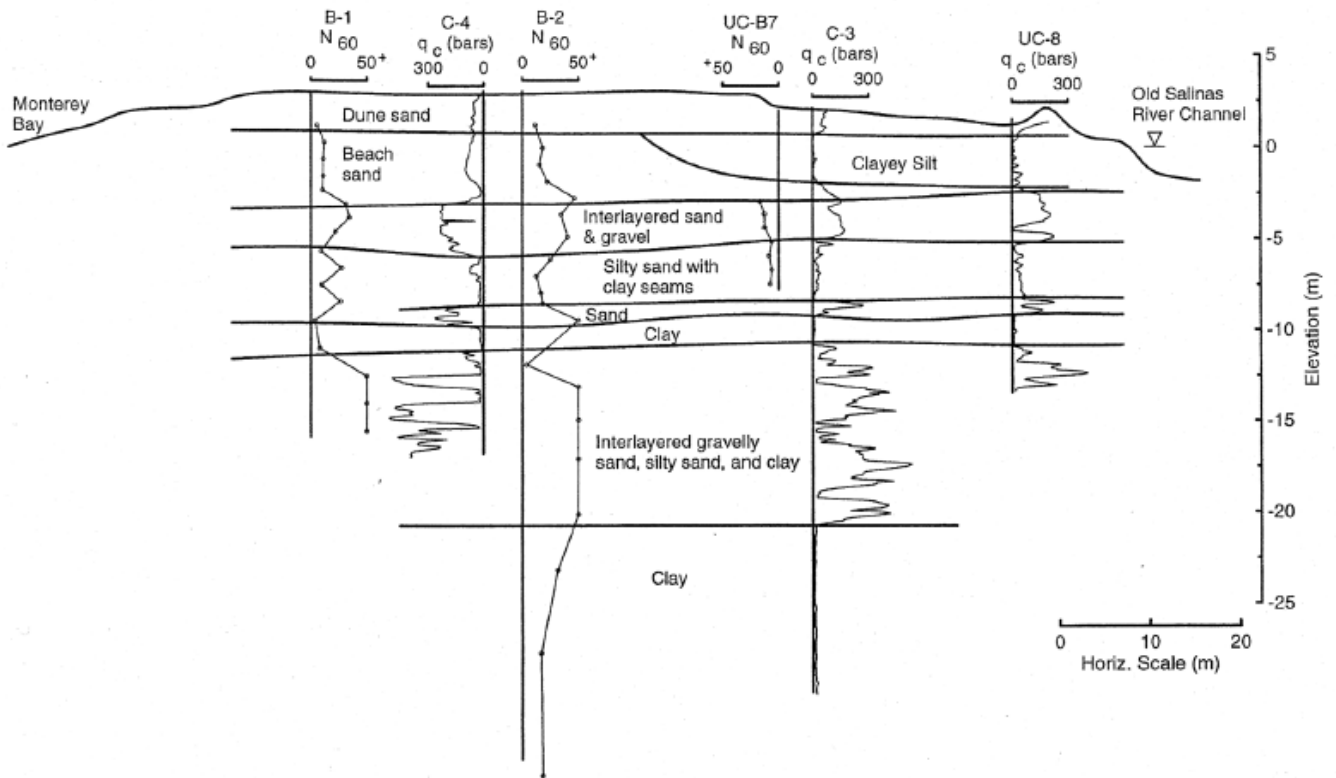


Fig. 6. Geologic section south of MLML facility (Section A-A' of Figures 4 and 8) (Boulanger et al. 1995).

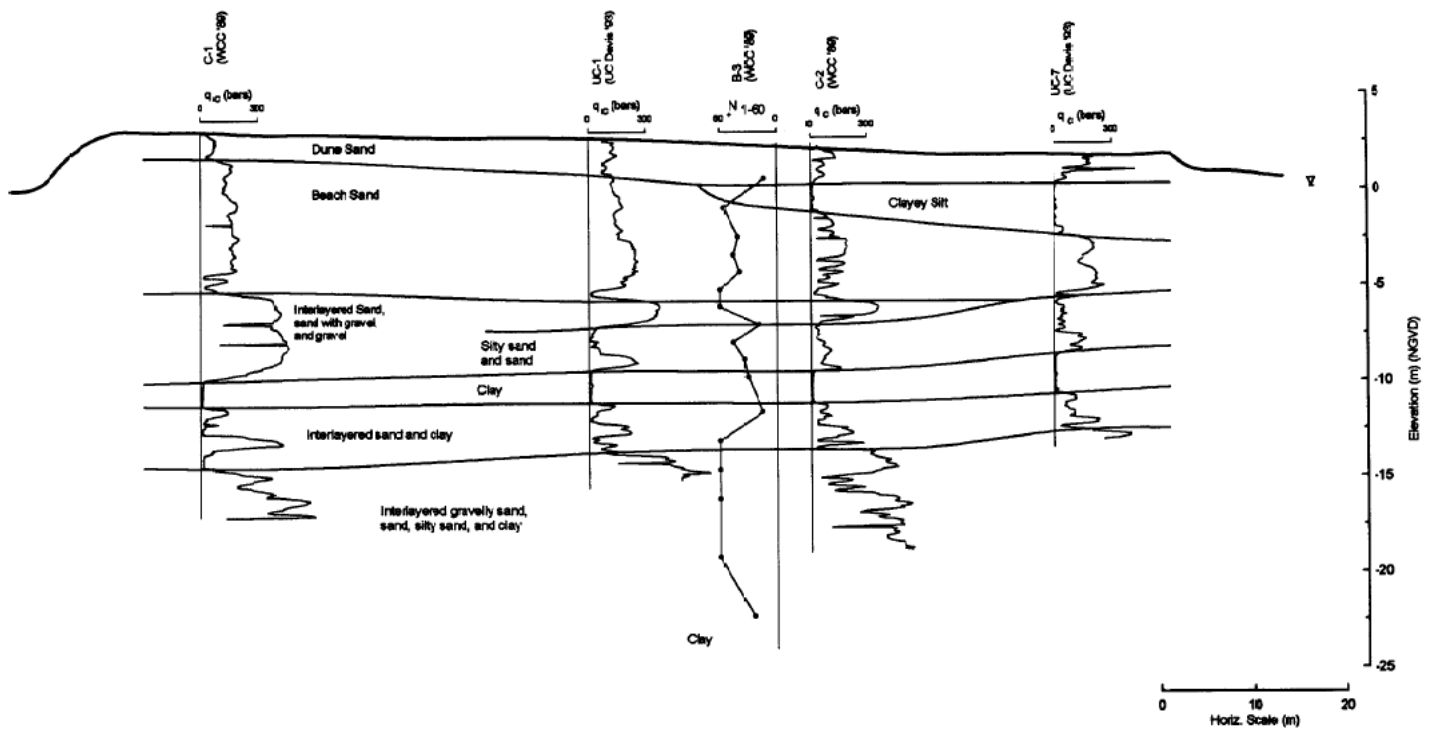


Fig. 7. Geologic section south of MLML facility (Section B-B' of Figure 8) (Boulanger et al. 1995).

Lateral spreading on the order of 0.75 m was estimated in the western direction, toward the Monterey Bay. Lateral spreading to the east toward the Old Salinas River was estimated to be 0.45 m at the structure and 0.8 to 1.4 meters east of Sandholdt Road (Figure 8). Overall, Boulanger et al. (1995) estimates spreading of the Moss Landing spit at the MLML facility to be about 1.4 m on the north side of the structure and 2.1 m on the south side of the structure. Vertical settlements were estimated at 0.35 m on the west side of the structure and 0.3 m on the east side. Some areas of heave were also observed at the site and are detailed on Figure 8.

Figure 8 shows contours of lateral displacement as predicted at Sections A-A' (Figure 9) and B-B' (Figure 10) as well as a plan view summary showing contours of predicted lateral displacement extrapolated from these sections overlain with measured values. Overall, lateral displacements were captured well as the calculated lateral spread displacements of the Moss Landing spit is approximately 2.25 m on the south side of the structure and 0.85 m on the north side of the structure. Predicted vertical displacements ranged from approximately 10 to 60 cm. Measured values of vertical displacements generally fall into this range.

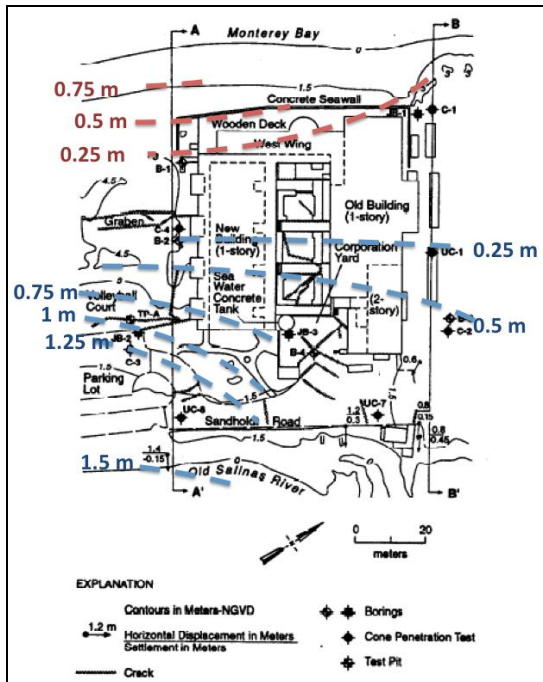


Fig. 8. Measured and predicted lateral deformations at the MLML Facility during the Loma Prieta Earthquake in 1989. Colored contours represent movement to the east (blue) and west (red).

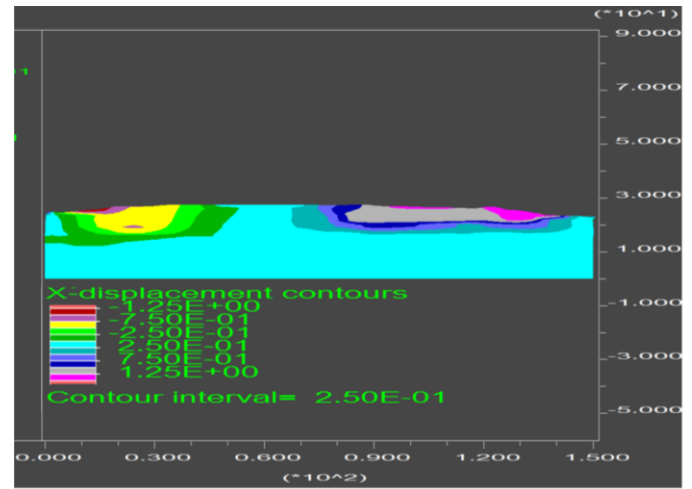


Fig. 9. Numerical model performed at Section A-A'.

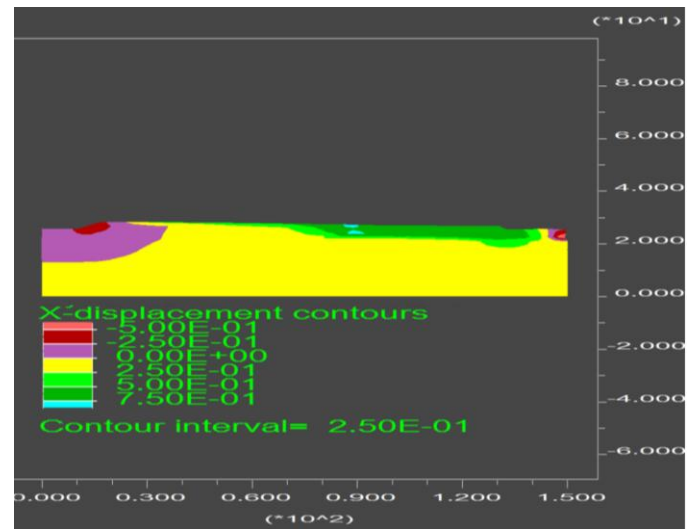


Fig. 10. Numerical model performed at Section B-B'.

SUMMARY AND CONCLUSIONS

Calibration of the fully nonlinear effective stress UBCSAND soil model using CSS test results established trends in the variation of its model parameters that prove useful for employing the UBCSAND model in practice. The CSS-based model parameter calibration led to the development of UBCSAND model parameterizations that were found to capture the observed performance of a well-documented liquefaction-induced displacement case history.

The UBCSAND model parameters are simplified to corrected SPT blowcount $((N_1)_{60})$, and two “fitting” parameters (i.e., m_{hfac1} and m_{hfac4}). The model parameters m_{hfac1} and m_{hfac2} were found to serve a similar function. Best results

were obtained by setting the parameters equal to one another. Values of 0.5 to 2.0 were typical values used in our analyses, though values can be higher and lower than this range of values. Non-plastic or low plasticity silts were found to follow a similar trend to clean sands, though these materials required a slightly higher value of m_{hfac1} (and m_{hfac2}) to capture their measured cyclic response. The UBCSAND m_{hfac3} parameter was not used in this study. Lastly, the UBCSAND m_{hfac4} parameter was found to vary between approximately 0.5 and 2.5 for sands with typical values being between 1.5 and 2.0. For silty soils, a value of 0.5 was selected for cases where the soil had a higher void ratio, and a value of 1.5 was selected for lower void ratio silty soils.

The UBCSAND model as implemented in FLAC proved to be a reliable tool for evaluating the effects of liquefaction in the foundation of a soil embankment. With some initial calibration effort to understand trends in the input parameters, the model was able to capture the deformations due to lateral spreading at the Moss Landing Marine Laboratory case history well. Our hope is that this independent evaluation of the capabilities of this soil constitutive model to capture inertially driven liquefaction-induced lateral spreads will enable practicing engineers to employ this model with confidence in evaluations of the seismic performance of earth structures situated atop potentially liquefiable soils.

ACKNOWLEDGEMENTS

Research was supported by the U. S. Geological Survey (U.S.G.S.), Department of Interior, under USGS award number G09AP00010. The financial support of the USGS is gratefully acknowledged. We would like to thank Dr. Nicholas Sitar, Dr. Shideh Dashti, Dr. Ben Mason, Katherine Jones, Roozbeh Grayeli, and Nick Oettle for their valuable input.

REFERENCES

Arulmoli, K., K. K. Muraleetharan, M. M. Hossain and L.S. Fruth [1992]. “*VELACS: Verification of Liquefaction Analysis by Centrifuge Studies. Laboratory Testing Program. Soil Data Report*”, The Earth Technology Corporation, Long Beach, CA.

Beaty, M. and P.M. Byrne [1998]. “An effective stress model for predicting liquefaction behavior of sand,” *Geotechnical Earthquake Engineering and Soil Dynamics III*, ASCE Spec. Pub. No. 75, Edited by Dakoulos, Yegian and Holz, ASCE, Reston, VA, Vol. 1, pp. 766-777.

Boulanger, R.W., I.M. Idriss and L.H. Mejia [1995]. “Investigation and evaluation of liquefaction related ground displacements at Moss Landing during the 1989 Loma Prieta earthquake”. *Technical Report UCD/CGM-95/02*, UC Davis Center for Geotechnical Modeling, UC Davis, Davis, California.

Idriss, I.M. and R.W. Boulanger [2008]. “*Soil Liquefaction During Earthquakes*”, EERI Monograph, Oakland, California.

Kammerer, A., J. Pestana and R. Seed [2002]. “Undrained Response of 0/30 Sand Under Multidirectional Cyclic Simple Shear Loading Conditions”. *Geotechnical Engineering Research Report No. UCB/GT/02-01*, University of California, Berkeley, July.

Martin, G.R. and M. Lew, [1999]. “*Recommended Procedures for Implementation of DMG Special Publication 117: Guidelines for Analyzing and Mitigating Liquefaction Hazards in California*”, Southern California Earthquake Center, University of Southern California, Los Angeles, California.

Park, S.S. and P.M. Byrne [2004]. “Stress densification and its evaluation”, *Canadian Geotechnical Journal*, Vol. 41, pp. 181-186.

Parrish, J.G. [2008]. “*Special Publication 117A – Guidelines for Analyzing and Mitigating Liquefaction Hazards in California*”, California Geological Survey, Sacramento, California.

Sancio, R.B. [2003]. “*Ground Failure and Building Performance in Adapazari, Turkey*”, Ph.D. dissertation, University of California, Berkeley, California.

Tinsley, J.C., III and W.R. Dupre [1992]. “Liquefaction hazard mapping, depositional faces, and lateral spreading ground failure in the Monterey Bay Area, Central California, during the 10/17/89 Loma Prieta Earthquake”. *Proceedings from the Fourth U.S.-Japan Workshop on Earthquake Resistant Design of Lifeline Facilities and Countermeasures Against Soil Liquefaction*, Volume I of NCEER-92-0019, pages 71 – 85, Buffalo, N.Y.

Wu, J. [2002]. “*Liquefaction Triggering and Post Liquefaction Deformations of Monterey 0/30 Sand under Uni-Directional Cyclic Simple Shear Loading*”. Ph.D. dissertation, University of California, Berkeley, California.